Applied Catalysis B: Environmental 239 (2018) 36–45

Contents lists available at ScienceDirect

Applied Catalysis B: Environmental

journal homepage: www.elsevier.com/locate/apcatb

Molecular interaction of heterogeneous catalyst in catalytic cracking process of vegetable oils: chromatographic and biofuel performance investigation

Nabel A. Negm*, Abdelrahman M. Rabie, Eslam A. Mohammed

Egyptian Petroleum Research Institute, 1-Ahmed El Zommer Street, Nasr city, Cairo, Egypt

ARTICLE INFO

Keywords:
Catalytic cracking
Alternative fuel
Viscosity
Sulfur content
Fuel properties

ABSTRACT

Catalytic cracking processes (CC) of non-edible vegetable oils (VOs) are considered efficient pathway to produce alternative energy sources to replace the fossil fuel. Castor oil (CO) and jatropha oil (JO) are the appropriate resources for biofuels because of their chemical structures and their hydrocarbon chains which are similar to fuel. This investigation was conducted to synthesize, characterize and evaluate acidic catalyst in the CC of castor and JO. The interaction between the oils and the catalyst was studied based on the brand of the produces biofuels. The effect of the concentration of the catalyst on the reaction product was studied including: viscosity, kinematic viscosity, pour point and cloud point. The results revealed that the prepared catalyst can catalyze the cracking reaction of the VOs and produce several grades of biofuels. The study displayed that the physical and fuel characteristics of the obtained biofuels are located within the ASTM specification limits. Also, the chemical nature of the cracked oil has a substantial impact on the composition of the achieved biofuel. The mechanisms of the CC processes of CO and JO were proposed. The physical and fuel properties of the achieved biofuels were discussed using their chromatographic analysis data.

1. Introduction

The motivation of researchers to seek alternatives energy was due to the fossil fuel depletion. Therefore, it is necessary to have alternative fuels of high efficiency, energy conservation and ecologically safe [1,2]. Non-edible VOs have recently got interested due to their renewable origins and environmental benefits. These renewable resources have the possibility to substitute the fossil fuels [3,4]. The widespread use of petroleum fuels to meet energy needs has a harmful influence on the atmospheric environment, including: sulfur dioxide, lead oxide, nitrogen oxides and other toxic gases [5,6]. VOs are the most significant sustainable sources of alternative energy as they are considered as a source of environmentally clean energy [7–9]. From chemical point of view, VOs are mixture of triglycerides bearing three fatty acid chains linked to glycerol base. VOs as raw materials are lack of nitrogen and sulfur compounds, which provides a reduction of hazardous releases to the atmospheric environment by ignition in engines.

There are several methods to produce biofuels using VOs as feed stocks such as; pyrolysis [8,9], transesterification reaction [10–14] and the CC process of non-edible VOs which gave engine hydrocarbon [1,15,16]. Transesterification process has some disadvantages such as; it requires blending with diesel fuel which is not economically attractive. Pyrolysis process (thermal decomposition) needs high temperature of 600–900 °C [17–19]. Several studies on the CC of VOs were reported during the recent years, regarding the yields and quality of the obtained biofuels using numerous categories of catalysts [20–22]. It was reported [23] that during the CC of VOs, gasoline was produced in an amount of 40 wt % of feedstock, 10–15 wt% propane–propylene and butane–butylene fractions.

CC process has various benefits such as; (i) its ease of application and its use in the engines, (ii) non-polluting nature because it does not Contains sulfur or nitrogen compounds in addition to being produced from a renewable source, (iii) the cost of production is lower than traditional methods, (IV) sustainable and biodegradable [24–26]. The CC process of VOs requires a temperature less than 450 °C and the ratio of the used catalyst to oil is very low [27,28]. The type and chemistry of the oils have important impact regarding the produced biofuel specifications. Benson et al. [29] studied CC path ways for unsaturated mono-, di-, and triolein on various acid catalysts. The main products of the CC process were aliphatic hydrocarbons (C_6–C_7) and alkyl substituted mono and bicyclic arenes; propylene and monocyclic arenes. The structure of fatty acids that form VO triglycerides is of considerable importance, since the group composition of cracking products depends on them. Dupain et al. [20] found that a relatively greater number of

Abbreviations: CC, catalytic cracking; VO, vegetable oil; JO, jatropha oil; CO, castor oil

* Corresponding author.
E-mail address: nabelnegm@hotmail.com (N.A. Negm).

https://doi.org/10.1016/j.apcatb.2018.07.070
Received 14 May 2018; Received in revised form 18 July 2018; Accepted 27 July 2018
Available online 29 July 2018
0926-3373/

double bonds in rapeseed oil triglycerides facilitated the formation of aromatic hydrocarbons. The produced gasoline and gases in the pyrolysis of oleic acid were high compared to stearic acid or rapeseed oil. Also, the produced aromatics in gasoline obtained from pyrolysis of stearic acid were low compared to the pyrolysis of rapeseed oil or oleic acid. In the CC of VOs, the products and their chemical composition are subjective to various factors, including reaction duration, temperature, rate of reactants flow and type of catalysts [30–33]. During CC of palm oil methyl esters to produce bio gasoline, it was shown that the distillate compounds contain C_5 – C_{11} structures [34]. With the help of a catalyst, the pyrolysis is performed at low conditions of temperature and pressure with enhanced products quality [35]. In recent years, various categories of catalysts have been investigated for the CC of different VOs [36]. Yigezu et al, reported different metal oxides such as MoO_3, Co_3O_4, V_2O_5, NiO, and ZnO) are useful in the CC of VOs with appropriate physical and fuel characteristics of the produced fuels. Also, the maximum conversion was achieved 87.6% [35]. Prado et al, investigated the catalytic and thermal pyrolysis of soybean oil and reported the formation of various varieties of alkenes, alkanes, alcohols, carboxylic acids, and aromatics. Also, calcined bauxite has demonstrated a beneficial catalyst than other CC catalysts because of its economic low cost and since it does not need chemical treatment to achieve its activation [36]. Now, it is critical to find a high-efficiency and low-cost catalyst to be applied in the CC of VOs. γ-alumina is considered one of the promising materials as a result of its high activity due to the presence of a large amount of Lewis acid sites within its chemical structure [37]; further, it has a high surface area, and thermally stable at high temperatures. In this investigation, γ-alumina was prepared and characterized using sufficient spectroscopic methods and was evaluated in CC reaction of CO and JO to obtain biofuels. The obtained biofuels were characterized and specified according ASTM specification and were compared to the fossil fuel. The effect of the process parameters was correlated to the different characteristics of the obtained biofuels.

2. Experimental

2.1. Materials

Aluminum nitrate ($Al(NO_3)_3{\cdot}9H_2O$) and sodium carbonate (Na_2CO_3) were pure chemicals (99.8%) supplied from Merck, Germany. Sodium hydroxide and nitric acid were analytical grades obtained from ADWIC chemicals company, Egypt. CO and JO were obtained by cold pressing of the dried seeds and were used after physical purification.

2.2. Preparation of CC catalyst (nano γ-Al_2O_3)

Hydrated aluminum nitrate ($Al(NO_3)_3{\cdot}9H_2O$) (25 g, 0.066 M) and sodium carbonate (Na_2CO_3)(10.38 g, 0.125 M) solutions in deionized water (600 mL) were mixed instantly drop wisely in 2 L round-bottom flask containing ethylene glycol (60 mL) dissolved in deionized water (400 mL) under stirring condition for 4 h until complete precipitation. The pH of the medium was adjusted in range of 8–9 using 0.1 N solution of HNO_3 or NaOH. The obtained precipitate was aged at 70 °C for 3 h, filtered off and washed several time using deionized water and then with ethanol followed by acetone to prevent Na^+ ions contamination. The obtained precipitate was then oven dried at 100 °C for 24 h followed by calcination in a programmable oven at 550 °C and heating rate of 2 °C min^{-1} for 5 h in air to obtain nano γ-Al_2O_3 powder [38]. The obtained catalyst was then placed in desiccator filled with CaO to remove the moisture form the catalyst environment before characterization.

2.3. Characterization of catalysts

XRD analysis of nano γ-Al_2O_3 was carried out using a Philips PW-1050-25 diffractometer fitted with PW-1965-40 and PW-2100-00 using goniometers employing Ni-filtered Cu. Ka radiation at 500 KV and 30 mA, in order to confirm the crystal structure. The scans were taken at 2θ = 4–80°. X-ray fluorescence (XRF) was recorded using a Bruker (S4 EXPLORER) operated at 20 mA and 50 kV. The Brunauer, Emmett, and Teller (BET) surface area of the catalysts was measured using Quanta chrome AS1Win, Quanta chrome Instrument v_2.01. Prior to such measurements, all samples were perfectly degassed at 200 °C for 6 h before experiments. The specific surface area (BET) was determined from the linear part of the adsorption curve. The pore diameter distribution was calculated from the desorption branch using BJH formula. FTIR analysis was performed using Nicolet IS-10 FTIR over the wave number 4000-400 cm^{-1}. Temperature-programmed desorption (TPD) studies were obtained using an adsorption unit Micromeritics, (Chemisorb-2705) equipped with TCD detector. 500.0 mg catalyst sample was pretreated under helium flow at 500 °C for 30 min and allowed it to cool up to 100 °C, and at this temperature the gas was switched to 5% NH_3 in helium with a flow rate of 20 mL/min for 30 min and subsequently purged with helium gas at 100 °C for 1 h to remove the physically adsorbed NH_3. NH_3-TPD curves were obtained at temperature range of 100–800 °C with a ramping rate of 10 °C/min and hold at 800 °C for 30 min.

2.4. CC experimental setup

The setup of the CC process was arranged as follows (Scheme 1) [19]: in 500 mL two necked flask equipped by mechanical stirrer and distillation tail connected to a glass reservoir, suitable amount (200 mL) of CO or JO were charged. Nano γ-Al_2O_3 was used at 0.2, 0.4, 0.6, 0.8 and 1% by weight compared to each oil and mixed well for 5 min at room temperature. The reaction mixture was allowed to thermal agitation for 4 h at 280 °C under nitrogen flow (5 mL/min) and stirring at 150 rpm. The obtained products were condensed and collected. The condensed biofuels (recorded) were settled in a separating funnel and then centrifuged to separate the produced water (recorded). The obtained vapors during the reactions were also collected to determine the efficiency of the reaction conversion. The reaction conversion (reaction effieicncy) was considered based on the amount of the condensed liquid in each reaction condition (catalyst amount) and was calculated as follows: efficiency = (liquid obtained/total amount of oil used) × 100.

2.5. Characterization of oil and biofuel

2.5.1. GC chromatographic measurements

GC-Chromatographic analysis of the oils and the different biofuel samples obtained at 1% catalyst ratio were analyzed using GC-7890A instrument equipped with DB-23 column, 60 mm × 0.25 mm, i.d. of 0.25 μm. For the biofuel components characterizaon, the temperature of

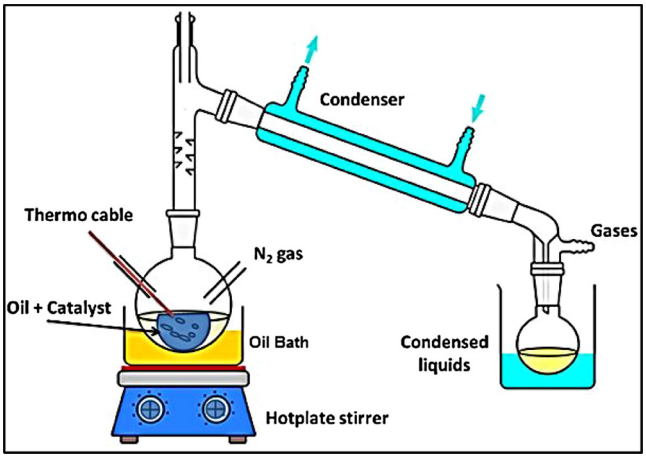

Scheme 1. Experimental setup of the catalytic cracking of the different oils.

the oven was programmed at 35 °C for 5 min. Then, the temperature was raised to 300 °C at a heating rate of 20 °C/min, while the temperature of the oven was retained at 300 °C for 20 min. The injection volume of the liquid sample was 0.1 mL, and helium (He) was used as a carrier gas at a flow rate of 1 mL/min. this analysis provided the fatty acid composition of the used oils and the hydrocarbon composition of the biofuels as well.

2.5.2. Density

Density (ρ) is defined as the mass (m) per unit volume (v) of the measured oil or biofuel using the following equation: $\rho = m / v$ (kg/m^3) according to the procedures described in ASTM D-4052 [39].

2.5.3. Kinematic viscosity

Viscosities of oil and biofuels were measured using the ASTM test method (D-445) [40]. In this method, the time was measured for a fixed volume of liquid to flow under gravity through the capillary of a calibrated viscometer under a reproducible driving head and at a closely controlled and known temperature. The kinematic viscosity was the product of the measured flow time and the calibration constant of the used viscometer.

2.5.4. Cloud point

The cloud point is defined as the temperature at which a cloud as wax crystals first appears in a liquid when it is cooled. Cloud point was measured according to (ASTM D-2500-91) [41] by cooling of clear sample and the temperature at which the opacity of the sample is disturbed was recorded. The test was repeated three times and the average of the three readings was considered.

2.5.5. Pour point

Pour point is defined as the maximum temperature at which the surface of the fluid could be tilted without any of the fluid pouring off. Pour point was measured according to ASTM standard method (D-97-11) [42], in brief; the oil sample was heated and then cooled at a specified rate and examined at intervals of 3 °C for flow characteristics. The lowest temperature at which movement of the specimen is observed is recorded as the pour point.

2.5.6. Acid value

The acid value is the number of milligrams of potassium hydroxide necessary to neutralize the free acids in 1 g of the oil. Acid value of the oil was determined according to the method of ASTM D-664 [43].

2.5.7. Oxidation stability

This test method determines resistance of oils and biofuels to oxidation when stored statically in an oxygen atmosphere in a sealed system at an elevated temperature under conditions of test. The oxidation stability was determined according to the method described in ASTM D-7462 [44].

2.5.8. Iodine value

The iodine value of oils is a measure of the unsaturated fatty acid content of that product and consequently a measure of the ease of oxidation or drying capacity of that oil. The iodine value was determined using ASTM test method of (D-5768) [45] for the used oils and the obtained biofuels.

2.5.9. Ash content

Ash content is inorganic residue that remains after combustion of the oil in air at specific high temperature. Ash content was measured according to ASTM D-482 standard [46]. The sample was contained in a suitable vessel, ignited and allowed to burn until ash and carbon remained. The carbonaceous residue was reduced to an ash by heating in a muffle furnace at 775 °C, cooled and weighed.

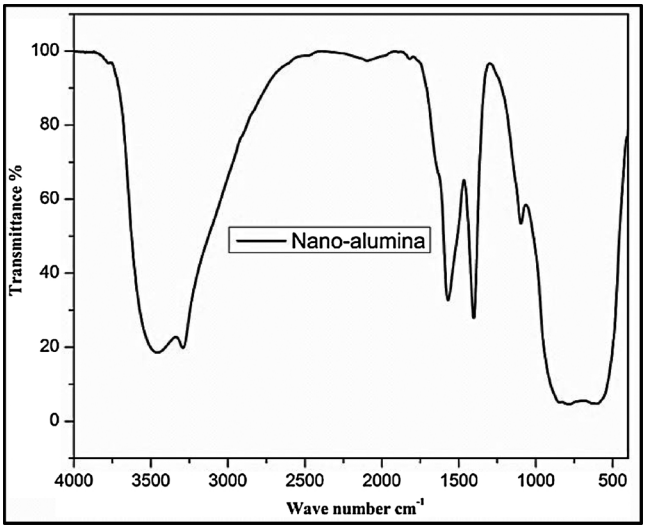

Fig. 1. FTIR spectra of the prepared Nano γ-alumina catalyst.

2.5.10. Sulfur content

Sulfur content was determined by using Energy Dispersive X-ray Fluorescence Spectrometry according to ASTM D-4294 [47]. This provided a measurement of the total sulfur in petroleum and petroleum products. Also, provides whether the sulfur content of the fuel meets specification or regulatory limits.

3. Results and discussion

3.1. Catalyst characterization

FTIR spectra of nanostructure of γ-Al_2O_3 are shown in Fig. 1. It is clear from the spectra the appearance of the vibrational bands of Al−OH and Al-O in the range of 3000–3600 cm^{-1}, while the stretching and bending vibration of hydrogen bonding OH groups at 1632 cm^{-1}. The peak appeared at 1080 cm^{-1} was assigned to Al-O-Al symmetric pending stretching vibrations [48]. The stretching vibration at 1560 cm^{-1} was assigned to Al−OH bond. The weak bands located in the absorption range of 1100–1200 cm^{-1} were attributed to Al-O [49].

The surface area and pore structure of the prepared nano γ-alumina catalysts were characterizes using N_2 adsorption-desorption measurements. The isotherm of adsorption-desorption is represented in Fig. 2,

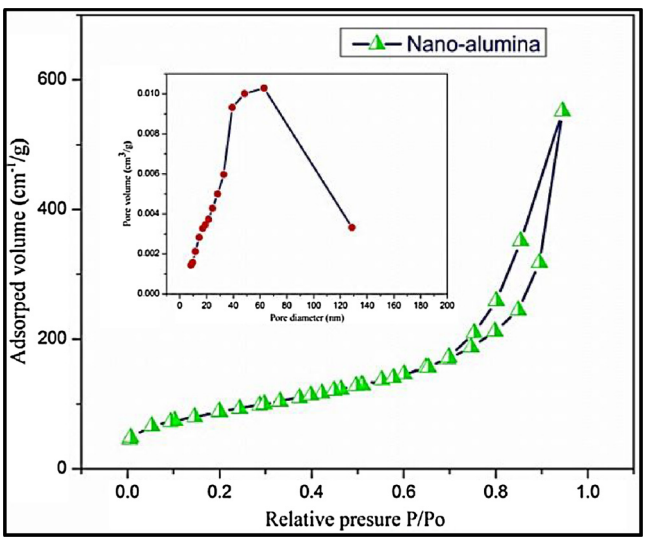

Fig. 2. N_2 adsorption-desorption of the prepared nano γ-alumina catalyst.

Table 1
Average surface area, pore volume and pore diameter of the prepared nano γ-alumina catalyst.

Surface area, ($m^2 g^{-1}$)	Total pore volume, ($cm^3 g^{-1}$)	Pore radius, (Å)
308.88	0.854	62.91

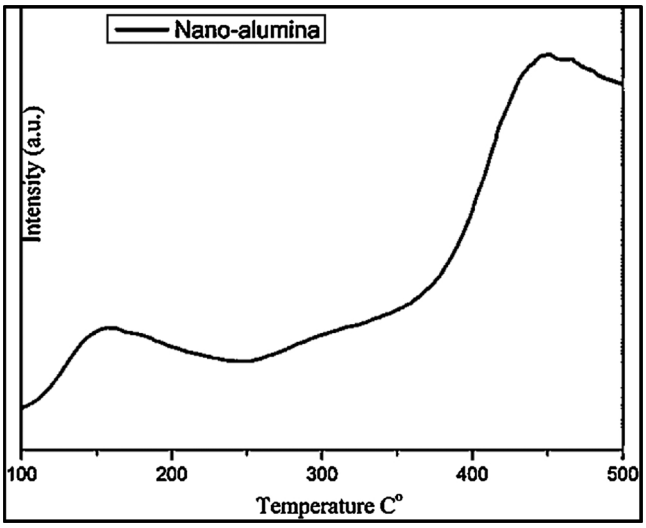

Fig. 3. Temperature programmed desorption (NH_3-TPD) of the prepared nano γ-alumina catalyst.

and the average pore size and pore volume were listed in Table 1. Alumina-free replicas show Type IV isotherms with a pronounced condensation step in the relative pressure (P/P_o) range of ~0.1–0.2 indicating narrow-sized mesopores. The N_2-uptake of the adsorption isotherms at P/P_o was > 0.8 and was associated with a second capillary condensation of nitrogen due large voids between the particles. The location of hysteresis loops among the adsorption and desorption branches of meso-alumina shows the presence of tubular pore structures or interconnected pores.

Ammonia adsorption-desorption (NH_3-TPD) measurements enable to determine the intensity and strength of the acidic sites (catalytic sites) of the catalyst surface. NH_3-TPD profile of the prepared nano-alumina catalyst is shown in Fig. 3. It was reported that γ-alumina shows predominant three types of OH groups [50]. The first is a terminal OH group attached to a single tetrahedral or octahedral Al atom ($OHAl_T$ or $OHAl_O$), the second is a bridging OH coordinated to two octahedral Al(OH_2Al_O) or tetrahedral-Al and octahedral-Al ($OHAl_OAl_T$), while the third is a bridging OH group which attached to three octahedral Al(OH_3Al_O) giving rise to acidic protons.

TPD studies of the prepared catalyst showed three types of the acidic sites: weak, medium and strong, expressed in terms of NH_3-mmol/g catalyst. The number of the different acid sites was calculated using TPD isotherm and listed in Table 2. It is clear that the total acid sites of the prepared catalyst 0.494 mmol/g, which are higher than the reported acid sites of the before reported γ-alumina catalyst which were varied between 0.355 mmol/g [51] and 0.445 mmol/g [52]. That showed the higher activity of the prepared nano γ-alumina catalyst which explain its higher catalytic activity in CC reaction of the studied oils.

Table 2
NH_3-TPD data of the prepared γ-alumina catalyst.

Number of acid sites (mmol NH_3/g catalyst)			
Weak	Medium	Strong	Total acid sites
0.049	0.005	0.44	0.494

Transmission electron microscopy (TEM) image of the prepared nano γ-alumina catalyst (Fig. 4a) shows disordered stacking nano-rod particles in the geometrical structure of the catalyst. Scanning electron microscopy (SEM) images of the nano γ-alumina catalyst (Fig. 4b) showed that the nanoparticles of γ-Al_2O_3 are formed of spherical nanosized aggregations with varied spherical sizes ranged between 3–6 nm as represented in Fig. 4b.

Fig. 5 shows the XRD patterns of the calcination product at 550 °C in air, and designates that γ-Al_2O_3 phase having spinel lattice [JCPDS File no. 29–63] and pure crystalline in nature. The calculated crystallite size (D) using Scherrer equation indicate their values within 3–5 nm. The broadening of the XRD peaks revealed the nanosize nature of γ-Al_2O_3 particles in these samples. XRD results reveal that the calcination produces well-crystallized γ-Al_2O_3 powders.where k is a constant ~0.9, λ is the wavelength of the X-rays, β is the full width of diffraction peak at half maximum intensity and Θ is the Bragg angle.

The particle size of the prepared nano γ-alumina catalyst obtained from TEM spectroscopy and XRD calculation were comparable to each other which proves the formation of the catalyst in the nano-size structure with particle size diameter range of 3–6 nm.

3.2. Vegetable oils and biofuel properties

The physical properties and acid profile of oils were determined and listed in Table 3. The fatty acids composition of the two oils were comparable to the published data with some minor differences refereeing to the region and season of the farming. JO has lower viscosity and density than CO which can be ascribed to the presence of high abundance of recinoleoic acid in CO which increases these two properties as a result of the presence of the hydroxyl group in its chemical composition. The high abundance of oleic and linoleic acid in the chemical composition of JO increases its iodine value (due to the comparatively higher unsaturation content) and also decreased its oxidation stability. Cloud point, pour point and sulfur content values were similar in the two oil.

The amount of the catalyst used were obtimized by gradual increasing the amount of the catalyst used from 0.2 to 1% and the reaction effieicny was calculated in each catalyst ratio using the amount of the obtained biofuel and the initial amount of oil used, Table 4. The obtained gases yield % was also calculated. It was observed that the amount of the condensed biofuel increased gradually by increasing the catalyst ratio to reach its maximum at 1% catalyst ratio.

Catalyst concentration was significantly influenced CC reaction of CO and JO to produce their corresponding biofuels. The acidic reactive sites in the used catalyst are responsible for the cracking reaction of the oils. Increasing the amount of the catalyst used increased the reactive area of the catalyst interacted by the oils, and also increased the number of the acidic active sites participated in the reaction [53]. The data in Table 4 revealed that the gradual increase in the catalyst amount from 0.2 to 1% increased the CC reaction efficiency from 85%–92% and 86%–94.5% for JO and CO, respectively. Further increase in the catalyst amount was increased the gases products and decreased the liquid products, which could be due to the accelerated cracking of the oils.

3.2.1. Density

The densities of the obtained biofuels from CC of JO and CO using the prepared catalyst at different ratios were determined. The obtained data represent two main characteristics. First, the densities of all the biofuels obtained from the cracking process are ranged between 0.8991–0.8976 g/cm^3 in case of CO biofuels, and 0.8989–0.8910 g/cm^3 in case of JO biofuels which are located within the ASTM range (0.9100 g/cm^3) [39]. Second, the densities of the biofuels are decreased by increasing the catalyst ratio to reach to the lower values (0.8965,

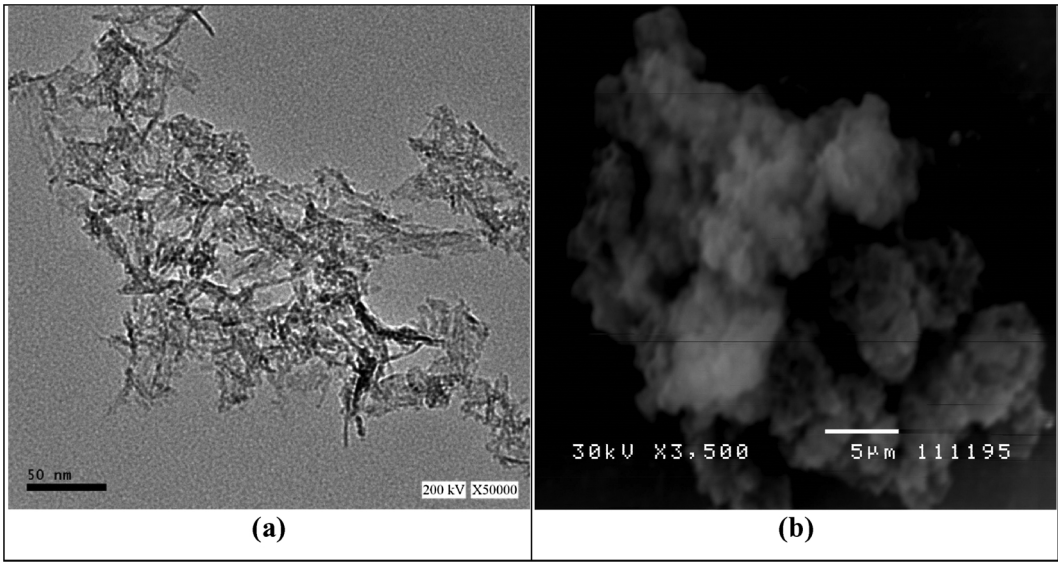

Fig. 4. HR-TEM (a) and SEM (b) of the prepared Nano γ-alumina catalyst.

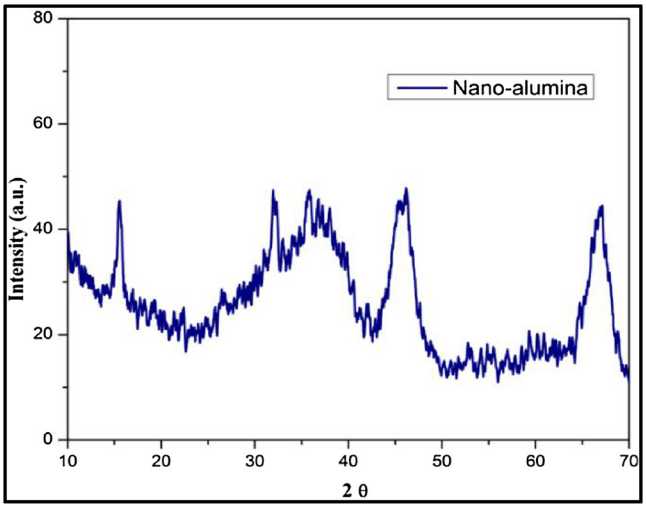

Fig. 5. XRD spectra of the prepared nano γ-alumina.

Table 3
Characterization of CO and JO.

Oil characteristics	CO	JO
Acid profile:	–	2.0
Myrestic acid (14:0)	2.0	15.0
Palmitic acid (16:0)	1.0	9.0
Stearic acid (18:0)	5.0	43.0
Oleic acid (18:1)	4.0	30.0
Linoleic acid (18:2)	85.0	–
Recinoleic acid (18:1, OH)		
Physical properties:	0.959	0.910
Density, 15 °C (g/cm^3)	43.0	37.0
Kinematic viscosity 40 °C, cSt	8	6
Cloud point, °C	4	2
Pour point, °C	0.02	0.08
Sulfur content, wt.%	2.8	3.70
Acid value, (mg KOH/g)	5.5	2.6
Oxidation stability, (h)	80.5	104.5
Iodine value, g I_2/100 g oil		

0.8910 g/cm^3 and 0.8979, 0.8976 g/cm^3, for jatropha and castor biofuels respectively) at 0.8 and 1% of the catalyst (Fig. 6). The increase in the catalyst ratio increases the number of the reactive sites which participate in the CC reaction that consequently increases the extent of the cracking reaction [54]. The increase in the catalytic reactive sites by increasing the catalyst ratio leads to successive cracking of the hydrocarbon chains and to produce short chain hydrocarbons compared to the long hydrocarbon chains in case of using catalyst ratio of 0.2 and 0.4%. The density of the oil used has a significant influence on the densities of the obtained biofuels. Table 3 revealed that CO is more dense than JO, which accompanied by higher densities of CO biofuels than JO biofuels. The high density of CO is attributed to the high abundance of recinoleic acid in CO (85%) which increases its viscosity due to the presence of the hydroxyl groups.

3.2.2. Kinematic viscosity

The determined values of kinematic viscosities of CO were 43 cSt and for JO was 37 cSt at 40 °C. It is clear that the two studied oils are highly viscous, due to the presence of long alkyl chains of oleic, linoleic and stearic acids in their triglyceride molecules [55]. It was reported that oils which have comparatively short fatty alkyl chains exhibited lower viscosities. Coconut oil has 44–52% of lauric acid and 13–19% myrestic acid and its average viscosity is 28 cSt, also pilu oil has 40–47% of lauric acid and 28–35% of myrestic acid and its average viscosity is 24 cSt [56]. Furthermore, higher unsaturated fatty acids oils have lower viscosities than lower unsaturated [57]. The comparatively higher viscosity of CO than JO is attributed to the presence of high ratio (85%) of unsaturated hydroxyl fatty acid (recinoleic acid). JO has high oleic and linoleic alkyl chains (oleic 44%, linoleic 32%) which explained its lower viscosity than CO. The values of kinematic viscosities of the obtained biofuels from the CC of JO and CO using different amounts of the prepared nano γ-alumina were measured at 40 °C (Fig. 7). It is clear from Table 3 and Fig. 7 that the viscosities of the obtained biofuels are lower than their corresponding oils. That is due to the cracking of the triglycerides chains and the formation of the corresponding alkyl chains of the different oil. The data also comprise that the viscosities of the biofuels obtained from cracking process of CO are comparatively higher than those obtained using JO. The higher viscosities in the biofuels are attributed to the nature of the obtained alkyl chains from the CC reactions.

The nature of the alkyl chains in the biofuels are differing by changing the ratio of the catalysts used. Increasing the alkyl chain length increases the viscosity of the compounds. The gradual increase in the catalyst ratio from 0.2% to 1% is gradually decreasing the kinematic viscosities of the obtained biofuels. That indicates the gradual decrease in the alkyl chain lengths of the obtained molecules by the gradual

Table 4
Reaction products, efficiency and sulfur and ash contents of the obtained biofuels.

Oil type	JO					CO					Specification limits
Catalyst ratio, wt.%	0.2	0.4	0.6	0.8	1	0.2	0.4	0.6	0.8	1	
Evolved gases (%)[a]	12%	12%	10%	9%	8%	12%	12%	10%	8%	5%	
Biofuel/ oil reacted	170/200	174/200	176/200	181/200	183/200	172/200	175/200	179/200	183/200	189/200	
Solids and carbon deposits	≈3%	≈1%	≈2%	≈1.5%	≈0.5	≈2%	≈0.50	≈0.5%	≈0.5	≈0.5	
Reaction efficiency	85%	87%	88%	90.5%	92%	86%	88%	89.5%	92.5%	94.5%	
Sulfur content, wt.%	0.011	0.009	0.008	0.005	0.001	0.016	0.012	0.011	0.009	0.002	< 0.01
Ash content, wt.%	Nil	Nil	Nil	Nil	Nil	Nil	Nil	Nil	Nil	Nil	< 0.01

[a] Evolved gases were collected and determined quantitavely.

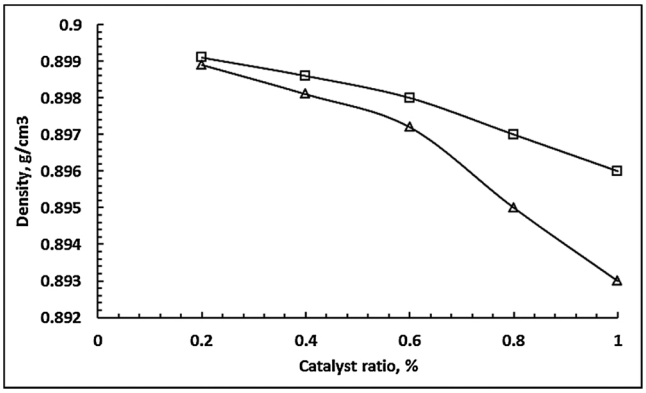

Fig. 6. Dependence of biofuels densities on the catalyst ratio used in cracking process (□: CO biofuel, Δ: JO biofuel).

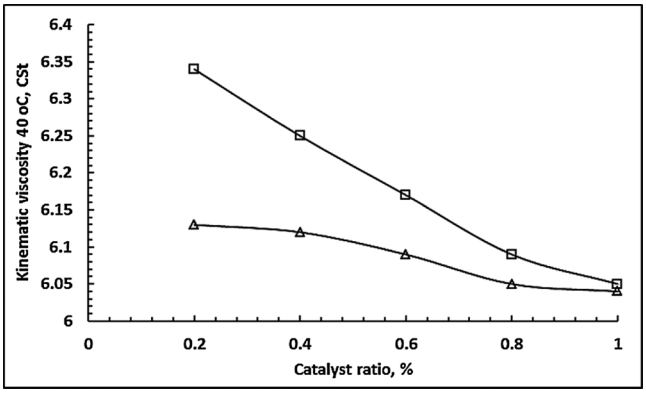

Fig. 7. Relationship between the kinematic viscosities of the obtained biofuels and the used catalyst ratio (□: CO biofuel, Δ: JO biofuel).

increase of the catalyst ratio. Increasing the amount of the used catalyst increases the cracking of the different oils and accelerates the cracking reaction. That enriches the obtained biofuels by shorter alkyl chains than the longer alkyl chains, consequently the viscosities decreased by increasing the catalyst amount [58]. The highest viscosities were 6.34, 6.25, 6.12 and 6.13 cSt at 40 °C obtained from CO and JO biofuels at 0.2% and 0.4% catalyst ratio, respectively. The lowest viscosities were obtained at 1% catalyst ratio for both oils. The nature of the used oil has an effective influence on the viscosity of the obtained biofuels. CO has higher viscosity than JO; hence the biofuels of the JO are characterized by low viscosities. The viscosities of the obtained biofuels using CO and JO during the CC reaction in the presence of nano γ-alumina catalyst were comparable [59] to the corresponding values of the biodiesel reported in the literature.

3.2.3. Cloud point and pour point

The cloud point and pour point of the biofuels are two important properties concerning the cold flow properties of the biofuels at elevated cold temperatures. Cloud point represents the point at which the clouds formed in the fuel matrix by decreasing the temperature. Pour point represents the temperature at which the fuel starts to solidify and lose its flow characteristics. It is clear that higher pour and cloud points decreases the fluidity of the biofuel and consequently plugging off the joints in the engines. The biodiesels have comparatively higher cloud and pour points due to the higher molecular weights and the fatty acid moieties in their chemical structures [60]. High cloud and pour points of commercial biodiesels can be modified by several methods, including: mixing by short chain alcohols [61], mixing by lighter hydrocarbons [62] and pyrolysis of oils. The pour points and cloud points of the prepared CO biofuel and JO biofuel were determined and represented graphically in Fig. 8. The data represented in Fig. 8 showed two main characteristics for the different biofuels. First, both pour points and cloud points of the different biofuels are decreased by increasing the catalyst ratio to reach the minimum at almost equal values for both types of biofuels at 1% catalyst ratio. Second, both cloud and pour point values of CO biofuels at the whole range of catalyst ratio are always higher than those for JO biofuels. That can be attributed to the nature of the two biofuels and their chemical compositions. It is clear also from data in Table 3 that the properties of the parent oils have a significant influence on the properties of their corresponding biofuels. CO has higher cloud and pour points and consequently its corresponding biofuels have higher values than JO biofuels as JO has the lowest values.

3.2.4. Flash point

The flash point of the biofuel is an important property determines its applicability, storage, and transportation conditions. The flash point of the biofuel determines its applicability in the specific engines, either as biodiesel or as bio-gasoline. The ASTM standard value of biodiesel is ranged between 130–150 °C, while bio-gasoline has standard ASTM value of flash point at 52 °C. The flash points of the obtained biofuels from the cracking reactions of CO and JO were determined, Table 4. Comparing the flash points of the different biofuels by the biodiesel and bio-gasoline showed that the obtained biofuels are categorized under bio-gasoline class.

The flash points of the different grades of the biofuels are ranged between 52–58 °C. That is in accordance with the ASTM standard value at minimum of 52 °C [63]. It was reported that the flash point of the biofuel is related to its chemical structure and mainly dependent on the alkyl chain length of the different components. Shorter alkyl chains exhibit low flash points and increased by the gradual increase of these chain lengths.

The determined flash points of the obtained biofuels were gradually decreased from 57 to 52 °C in case of JO biofuels; while were in the range of 58-54 °C in case of CO biofuels. The flash points of the biofuels were decreased by increasing the catalyst ratio. Increasing the catalyst ratio has a considerable effect on the alkyl chain length of the obtained hydrocarbons in the different biofuels. That can be attributed to the increase of the reactive sites in the catalysts which participated in the

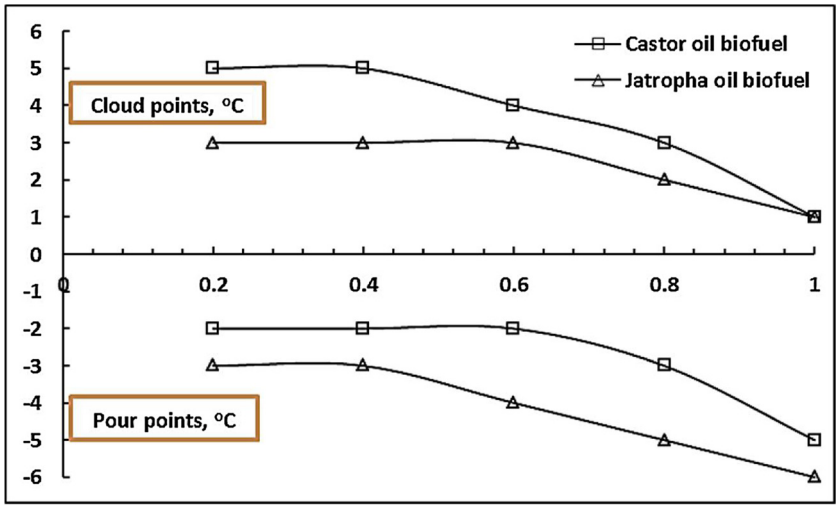

Fig. 8. Variation of pour point and cloud point of the biofuels on the catalyst ratio.

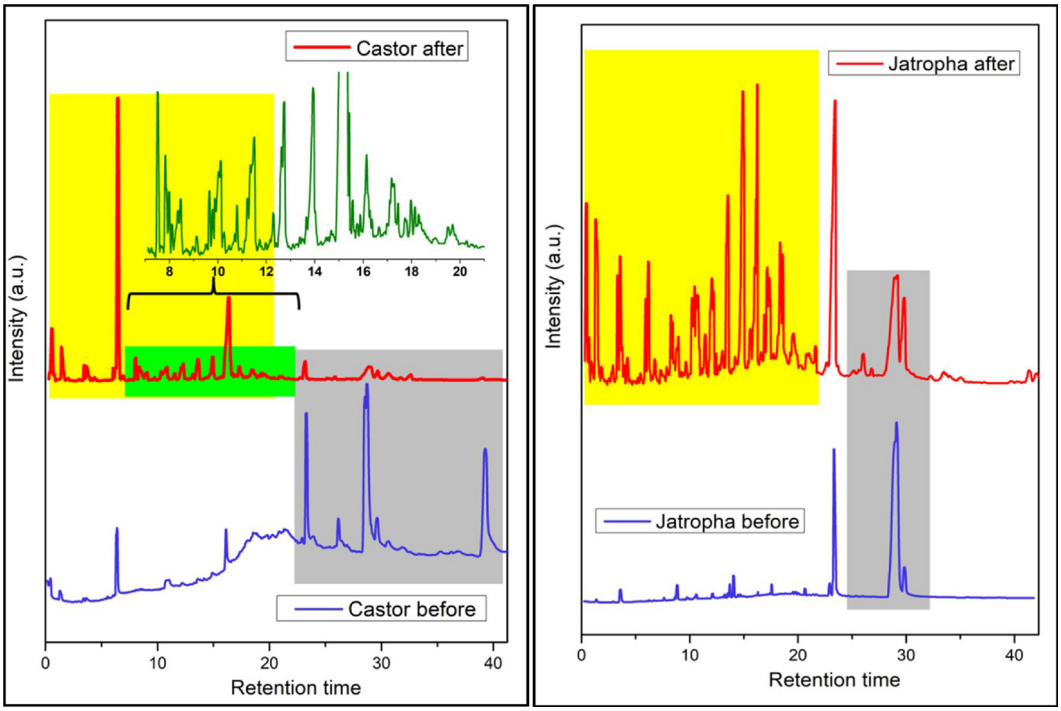

Fig. 9. Chromatographic analysis of: a. CO and CO biofuel, b. JO and JO biofuel.

CC process by increasing the amount of the catalyst. Consequently, the quality of the biofuel can be controlled by changing the ratio of the catalyst used during the cracking process.

3.2.5. Sulfur content

The total sulfur content in the VOs is an important parameter which determines for large extent the amount of sulfur in the final biofuel obtained from these oils. The sulfur in the VOs comes from some biochemical incorporated in the oils and their ratios depend on the origin and nature of these biochemical. The sulfur containing compounds in the VOs are mainly phospholipids and glucosinolates. They are the organic compounds derived from glucose and amino acids containing sulfur and nitrogen [64]. In JO, some components containing sulfur such as phospholipids and glucosinolates are presented in the ratio of 0.05% by weight [65]. In CO, the sulfur compounds are mainly glucosinolates with abundance 8 μmole/g. The comparatively higher content of sulfur in CO requires sensitive monitoring for sulfur in the produced biofuels. The total sulfur content in JO was determined as 0.02% by weight and it was 0.08% in CO. The produced biofuels from the different CC processes of the two oils using the synthesized catalyst showed considerable lowering in their sulfur content, Table 4. It is clear from the data in Table 4 that the sulfur contents of the different biofuels are located under the range of ASTM specification limit (0.1% by weight). Also, the sulfur content of CO biofuels are comparatively higher than that of JO biofuels, which related to the nature and abundance of sulfur containing compounds in the two oils.

The catalyst ratio has a great influence on the sulfur content in the obtained biofuel. It is clear that the gradual increase in the catalyst ratio from 0.2% to 1% is gradually decreasing the sulfur content in the biofuels from the two oils. Also, the results were in accordance by the initial sulfur content in the oils used. The decrease in the sulfur content by increasing the catalyst ratio was attributed to the cracking of the sulfur containing compounds in the oils and their decomposition into SO_x gases which evaporated during the process [66]. Higher catalyst

ratio increases the decomposition of these compounds and consequently decreases the sulfur content.

3.3. Chromatographic analysis of produced biofuel

The obtained biofuels from the CC process of CO and JO using the synthesized nanostructured γ-Al_2O_3 were promising due to the reactions were proceeded at product ratio ranged between 85–94% depending on the catalyst ratio. Also, the biofuels were obtained at comparatively lower temperatures of 280–320 °C which is lower than the temperatures ever reported in the literatures.

The chromatographic charts of CO and JO were represented in Fig. 9. It is clear from the values of the retention time of oils that CO fractions have higher retention times at 9, 16, 25, 29 and 40 min corresponding to palmitic, stearic, oleic, linoleic and recinoleic acids. Also their intensities are comparable to their abundance in the CO. Additionally, JO fractions located in the chromatographic chart at low retention times of 6, 9, 16, 25 and 29 min corresponds to myrestic, palmitic, stearic, oleic and linoleic acids at comparable intensities to their abundance in the JO. The average carbon distribution of the obtained hydrocarbons in the obtained biofuels from th cracking process in the presence of 1% catalyst ratio are represented in Table 5. The data represented in Fig. 9 showed that CO biofuel has higher fractions of long chain fatty acids than those found in JO biofuel.

The chromatographic study of the obtained biofuels showed varied behaviors than their corresponding oils. Obviously, the characteristic signals of both oils at 23, 29 and 40 min for CO and 23 and 29 min for JO were considerably decreased after the cracking process. The decreases in the characteristic oil signals indicates the cracking of the fatty acid moieties of oleic, linoleic and recinoleic acids in CO and oleic and linoleic acids in JO into shorter chains. The appearance of several signals at shorter retention times by high intensities referred to the short chain hydrocarbons formed during the reaction. Also, the appearance of the multiple signals at lower and narrow retention times indicated the formation of short chain hydrocarbon isomers.

Comparing between the chromatographic profiles of the obtained biofuels (Fig. 9) revealed that the hydrocarbon fractions of the CO biofuel are appeared at higher retention times than the retention times of the hydrocarbon fractions of JO biofuel. That showed the nature of the two biofuels obtained from the CC process. CO biofuel has longer hydrocarbon chains as represented from their comparatively higher retention times, while JO biofuel has shorter hydrocarbon chains as a result of shorter retention times. Furthermore, Fig. 9 revealed that the castor biofuel has several types and lengths of hydrocarbon chains. Translating the retention times into average hydrocarbon chains in the obtained biofuels revealed that the JO biofuel has higher content of short chain hydrocarbons in the range of C_5-C_{12} at 45.65% compared with 40.71% in case of CO biofuel. The middle hydrocarbon chains in the range of C_{12}-C_{16} were 27.94% in JO biofuel and 32.39% in case of CO biofuel. The higher hydrocarbon chains at > C_{18} chains were 22.5% in CO biofuel and decreased to 18.41% in case of JO biofuel, Table 5.

The large varieties of the obtained fractions in CO biofuel are due to the high abundance of the recinoleic acid in the oil. The presence of the hydroxyl groups in the recinoleic acid accelerates its cracking during the cracking process. The reaction is preceded by formation of free radical mechanism which accompanied by chain splitting to produces several reactive free radicals. The free radicals are undergoing chain termination, combination and cyclization leading to formation of several hydrocarbon isomers. That decreases the low hydrocarbon chains a represented in the values of C_5-C_{12} hydrocarbons. The recinoleate moieties also undergoes decarboxylation reaction to produce carbon dioxide and either unsaturated chains or free radicals which produces higher abundance of medium and higher hydrocarbon chain lengths in the range of C_{12}–C_{16} and > C_{18} fractions, Table 5 and Scheme 2. That is responsible for the formation of several isomers which appeared at the chromatographic chart.

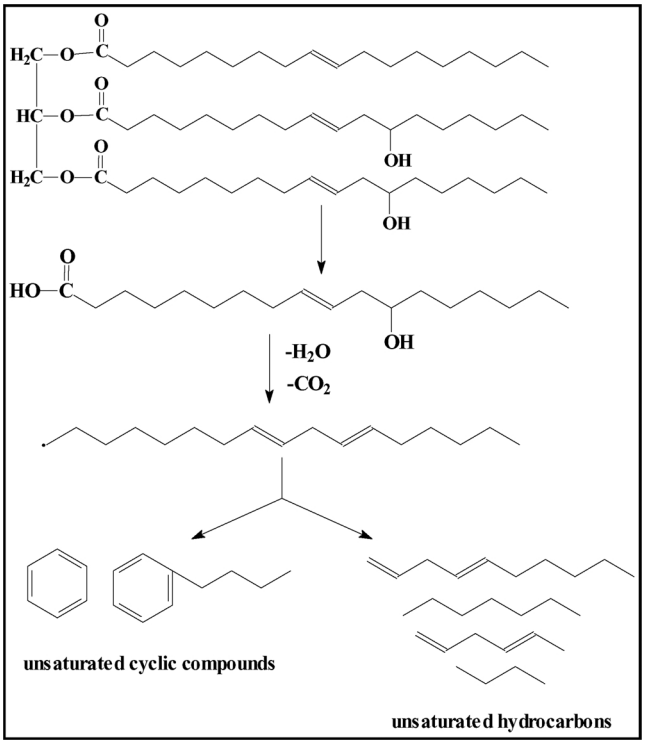

Scheme 2. CC pathway of CO.

In JO, oleic and linoleic acids are the main components in its chemical structure with the unsaturated sites as reactive cracking centers. That produces limited types of reactive free radicals which lead to formation of open chain saturated and unsaturated hydrocarbons with short chains and lower number of carbon atoms as shown in Scheme 3. That increses the abundance of the low molecular weight hydrocarbon chains in C_5–C_{12} range to 45.65% and decreases the medium and high hydrocarbon fractions compared to CO biofuel fractions. The formation of aromatic hydrocarbons may be limited in case of JO cracking may be due to the nature of the formed free radicals formed during the cracking reaction as represented in Scheme 3.

It was reported that the heat content and ignition properties of CO biofuels are more efficient than several VOs such as JO, olive oil, palm oil [67,68]. That was attributed to the cyclic and aromatic hydrocarbons formed during the production of biofuel from CO. The cyclization reaction during the cracking of the CO leads to the production of aromatic and unsaturated hydrocarbons which improve the quality of the biofuel and increases its heat content and ignition properties in engines.

The chromatographic study showed that the CO biofuel has higher hydrocarbon content with higher hydrocarbon chain lengths in the range of C_{16}-C_{18} and > C_{18}, while in case of JO biofuels the hydrocarbon content with higher chains were decreased considerably and the

Table 5
Average carbon distribution of the hydrocarbons obtained from CC of JO and CO using 1% catalyst ratio.

Biofuel type	C_5-C_{12} (%)	Retention time range, min	C_{12}-C_{16} (%)	Retention time range, min	> C_{16} (%)	Retention time range, min
Castor oil biofuel	40.71	8–14	32.39	14–18	22.50	18–40
Jatropha oil biofuel	45.65	8–14	27.94	14–18	18.41	18–29

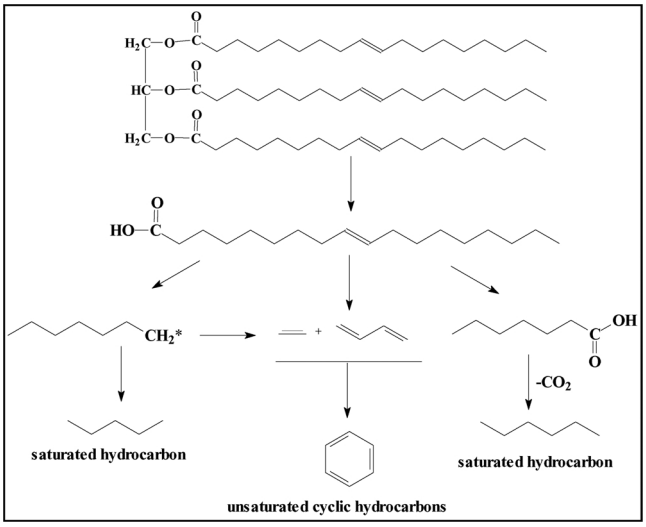

Scheme 3. CC pathway of JO.

lower hydrocarbon chains of C_5-C_{12} wer increased considerably. That explains the higher properties of CO biofuel, e.g., densities and viscosities, than the determined densities and viscosities of the hydrocarbons formulating the JO biofuel.

4. Conclusions

In conclusion, we prepare nano γ-alumina as a catalyst for catalytic cracking of castor oil and jatropha oil to prepared environmentally friendly biofuel to replace the fossil fuel. The catalyst was characterized by using TEM and XRD spectroscopy, Brunauer, Emmett, and Teller (BET), FTIR analysis, and Temperature-programmed desorption (TPD). The nano structures of the prepared catalyst were in narrow range of 3–6 nm. The catalytic cracking process of the vegetable oils using the prepared catalyst produced suitable biofuel according to ASTM specifications. The process efficiency was increased by increasing the catalyst concentration to 1%. The chromatographic analysis showed the effect of the oil type on the biofuel obtained, and the mechanism of the cracking process pathway was proposed. We believe that the prepared catalyst will make a new route in efficient catalytic cracking of vegetable oils to produce alternative and suitable source of green energy to have an impact the energy state to decrease the green house effect.

References

[1] A. Heydari, A. Askarzadeh, Techno-economic analysis of a PV/biomass/fuel cell energy system considering different fuel cell system initial capital costs, Sol. Energy 133 (2016) 409–420.
[2] A. Elfadly, I. Zeid, F. Yehia, M. Abouelela, A. Rabie, Production of aromatic hydrocarbons from catalytic pyrolysis of lignin over acid-activated bentonite clay, Fuel Process. Technol. 163 (2017) 1–7.
[3] C. Li, J. Ma, Z. Xiao, S.B. Hector, R. Liu, S. Zuo, X. Xie, A. Zhang, H. Wu, Q. Liu, Catalytic cracking of Swida wilsoniana oil for hydrocarbon biofuel over Cu-modified ZSM-5 zeolite, Fuel 218 (2018) 59–66.
[4] N. Mansir, Y.H. Taufiq-Yap, U. Rashid, I.M. Lokman, Investigation of heterogeneous solid acid catalyst performance on low grade feedstocks for biodiesel production: a review, Energy Convers. Manag. 141 (2017) 171–182.
[5] F.A. Rahman, M.M.A. Aziz, R. Saidur, W.A.W.A. Bakar, M. Hainin, R. Putrajaya, N.A. Hassan, Pollution to solution: capture and sequestration of carbon dioxide (CO2) and its utilization as a renewable energy source for a sustainable future, Renew. Sustain. Energy Rev. 71 (2017) 112–126.
[6] N. Kilinc-Ata, The evaluation of renewable energy policies across EU countries and US states: an econometric approach, Energy Sustain. Dev. 31 (2016) 83–90.
[7] A. Demirbas, Progress and recent trends in biofuels, Prog. Energy Combust. Sci. 33 (2007) 1–18.
[8] A. Demirbas, Biofuels securing the planet's future energy needs, Energy Convers. Manag. 50 (2009) 2239–2249.
[9] A. Demirbas, Biodiesel production from vegetable oils via catalytic and non-catalytic supercritical methanol transesterification methods, Prog. Energy Combust. Sci. 31 (2005) 466–487.
[10] G. Adebayo, O. Ameen, Physicochemical properties of biodiesel produced from Jatropha curcas oil and fossil diesel, J. Microbiol. Biotechnol. Res. 1 (2017) 12–16.
[11] L.F. Chuah, J.J. Klemeš, S. Yusup, A. Bokhari, M.M. Akbar, A review of cleaner intensification technologies in biodiesel production, J. Clean. Prod. 146 (2017) 181–193.
[12] B.R. Vahid, M. Haghighi, Biodiesel production from sunflower oil over MgO/$MgAl_2O_4$ nanocatalyst: Effect of fuel type on catalyst nanostructure and performance, Energy Convers. Manag. 134 (2017) 290–300.
[13] L.F. Chuah, J.J. Klemes, S. Yusup, A. Bokhari, M.M. Akbar, Z.K. Chong, Kinetic studies on waste cooking oil into biodiesel via hydrodynamic cavitation, J. Clean. Prod. 146 (2017) 47–56.
[14] A.A. Silva, D.S. Oliveira, F.R. Fernandes, A.G. Santos, V.P. Caldeira, L.D. Souza, Catalytic cracking of sunflower oil under Zr catalysts using thermogravimetry, J. Therm. Anal. Calorim. 131 (2018) 643–651.
[15] D.P. Serrano, J.A. Melero, G. Morales, J. Iglesias, P. Pizarro, Progress in the design of zeolite catalysts for biomass conversion into biofuels and bio-based chemicals, Catal. Rev. 60 (2018) 1–70.
[16] D.Y. Leung, X. Wu, M. Leung, A review on biodiesel production using catalyzed transesterification, Appl. Energy 87 (2010) 1083–1095.
[17] F. Ma, M.A. Hanna, Biodiesel production: a review, Bioresour. Technol. 70 (1999) 1–15.
[18] L. Meher, D.V. Sagar, S. Naik, Technical aspects of biodiesel production by transesterification-a review, Renew. Sustain. Energy Rev. 10 (2006) 248–268.
[19] M. Borges, L. Diaz, Recent developments on heterogeneous catalysts for biodiesel production by oil esterification and transesterification reactions: a review, Renew. Sustain. Energy Rev. 16 (2012) 2839–2849.
[20] X. Dupain, D.J. Costa, C.J. Schaverien, Appl. Catal. B: Environ. 72 (2007) 44.
[21] P. Tamunaidu, S. Bhatia, Bioresour. Technol. Rep. 98 (2007) 3593.
[22] T.L. Chew, S. Bhatia, Bioresour. Technol. Rep. 100 (2009) 2540.
[23] J.A. Melero, M.M. Clavero, G. Calleja, Energy Fuels 24 (2010) 707.
[24] A. Demirbas, Biodiesel, Springer, 2008.
[25] A. Kumar, S. Sharma, Potential non-edible oil resources as biodiesel feedstock: an Indian perspective, Renew. Sustain. Energy Rev. 15 (2011) 1791–1800.
[26] F.A. Twaiq, A. Mohamad, S. Bhatia, Performance of composite catalysts in palm oil cracking for the production of liquid fuels and chemicals, Fuel Process. Technol. 85 (2004) 1283–1300.
[27] F.A. Twaiq, A.R. Mohamed, S. Bhatia, Liquid hydrocarbon fuels from palm oil by catalytic cracking over aluminosilicate mesoporous catalysts with various Si/Al ratios, Microporous Mesoporous Mater. 64 (2003) 95–107.
[28] T.J. Benson, R. Hernandez, W.T. French, J. Mol. Catal. A Chem. 303 (2009) 117.
[29] J.D. Adjaye, S.P.R. Katikeni, N.N. Bakhshi, Catalytic conversion of biofuel hydrocarbons:effect of HZSM-5 and silica-alumina catalysts on product distribution, Fuel Process. Technol. 48 (1996) 115–143.
[30] F.A.A. Twaiq, N.A.M. Zabidi, A.R. Mohamed, S. Bhatia, Catalytic conversion of palm oil over mesoporous aluminosilicate MCM-41 for the production of liquid hydrocarbon fuels, Fuel Process. Technol. 84 (2003) 105–121.
[31] W. Charusiri, T. Vitidsant, Kinetic study of used vegetable oil to liquid fuels over sulfated zirconia, Energy Fuels 19 (2005) 1783–1789.
[32] M. Nasikin, A. Wahid, Perengkahan Metil Ester menjadi Biogasoline dengan Katalis Zeolite Alam, Prosiding Seminar Nasional Fundamental dan aplikasi Teknik Kimia, Institut Teknologi Sepuluh November Surabaya Nopember (2005) (In Indonesian).
[33] A. Widayat, Pembuatan Bahan Bakar Biodiesel Dengan Proses Perengkahan Berkatalis Zeolit Dan Bahan Baku Minyak Goreng Berahan Dasar Crude Palm Oil, Prosiding Seminar Nasional Fundamental Dan Aplikasi Teknik Kimia, Institut Tekonologi Sepuluh Nopember Surabaya, Nopember (2005) (In Indonesian) (2005).
[34] Sd. Grecco, D.R. Carvalho, C.H. Zandonai, N.R. Machado, L.M. Lião, E.A. González, M. Rangel, Catalytic cracking of crude soybean oil on Beta nanozeolites, J. Mol. Catal. A Chem. 422 (2016) 89–102.
[35] Z.D. Yigezu, K. Muthukumar, Catalytic cracking of vegetable oil with metal oxides for biofuel production, Energy Convers. Manag. 84 (2014) 326–333.
[36] C.M. Prado, N.R. Filho, Production and characterization of the biofuels obtained by thermal cracking and thermal catalytic cracking of vegetable oils, J. Anal. Appl. Pyrolysis 86 (2009) 338–347.
[37] A. Erkiaga, G. Lopez, M. Amutio, J. Bilbao, M. Olazar, Steam gasification of biomass in a conical spouted bed reactor with olivine and γ-alumina as primary catalysts, Fuel Process. Technol. 116 (2013) 292–299.
[38] I.N. Mukhambetov, S.R. Egorova, A.N. Mukhamed, A.A. Lamberov, Hydrothermal modification of the alumina catalyst for the skeletal isomerization of n-butenes, Appl. Catal. A Gen. 554 (2018) 64–70.
[39] ASTM International, D 4052: Standard Test Method for Density, Relative Density, and Gravity of Liquids, (2013).
[40] ASTM International, D-445: Standard Test Method for Kinematic Viscosity of Transparent and Opaque Liquids, (2000).
[41] ASTM International, D-2500: Standard Test Method for Cloud Point of Petroleum Products, (2007).
[42] ASTM International, D97-11: Standard Test Method for Pour Point of Petroleum Products, (2011).
[43] ASTM International, D-664: Standard Test Method for Acid Value of Petroleum Products, (2011).
[44] ASTM International, D-7462: Standard Test Method for Oxidation Stability of Biodiesel (B100) and Blends of Biodiesel With Middle Distillate Petroleum Fuel, (2016).
[45] ASTM International, D-5768: Standard Test Method for Determination of the Iodine Value of Fats and Oils, (2014).
[46] ASTM International, D-482: Standard Test Method for Ash Determination From Petroleum Products, (2013).

[47] ASTM International, D-4294: Standard Test Method for Sulfur in Petroleum and Petroleum Products by Energy Dispersive X-ray Fluorescence Spectrometry, (2015).
[48] P. Colomban, Raman study of the formation of transition alumina single crystal from protonic β/β ″aluminas, J. Mater. Sci. Lett. 7 (1988) 1324–1326.
[49] A. Vazquez, T. Lopez, R. Gomez, A. Morales, O. Novaro, X-ray diffraction, FTIR, and NMR characterization of sol–gel alumina doped with lanthanum and cerium, J. Solid State Chem. 128 (1997) 161–168.
[50] J. Peri, A model for the surface of γ-alumina, J. Phys. Chem. 69 (1965) 220–230.
[51] S. Karnjanakom, G. Guan, B. Asep, X. Du, X. Hao, J. Yang, C. Samart, A. Abudula, A green method to increase yield and quality of biooil: ultrasonic pretreatment of biomass and catalytic upgrading of bio-oil over metal (Cu, Fe and/or Zn)/γ-Al_2O_3, RSC Adv. 5 (2015) 3494–83503.
[52] A.M. Elfadly, A.M. Badawi, F.Z. Yehia, Y.A. Mohamed, M.A. Betiha, A.M. Rabie, Selective nano alumina supported vanadium oxide catalysts for oxidative dehydrogenation of ethylbenzene to styrene using CO_2 as soft oxidant, Egypt. J. Petrol. 22 (2013) 373–380.
[53] S.H. Teo, M. Goto, Y.H. Taufiq-Yap, Biodiesel production from Jatropha curcas L. oil with Ca and La mixed oxide catalyst in near supercritical methanol conditions, J. Superscript Fluids 104 (2015) 243–250.
[54] A.M. Rabie, E.A. Mohammed, N.A. Negm, Feasibility of modified bentonite as acidic heterogeneous catalyst in low temperature catalytic cracking process of biofuel production from nonedible vegetable oils, J. Mol. Liq. 254 (2018) 260–266.
[55] G. Knothe, K.R. Steidley, Kinematic viscosity of biodiesel fuel components and related compounds. Influence of compound structure and comparison to petrodiesel fuel components, Fuel 84 (2005) 1059–1065.
[56] A. Sarma, D. Konwer, P.K. Bordoloi, A comprehensive analysis of fuel proper- ties of biodiesel from koroch seed oil, Energy Fuels 19 (2005) 656–657.
[57] N.U. Soriano, V.P. Migo, K. Sato, M. Matsumura, Crystallization behavior of neat biodiesel and biodiesel treated with ozonized vegetable oil, Eur. J. Lipid Sci. Technol. 107 (2005) 689–696.
[58] N.A. Negm, G.H. Sayed, O.I. Habib, F.Z. Yehia, E.A. Mohamed, Heterogeneous catalytic transformation of vegetable oils into biodiesel in one-step reaction using super acidic sulfonated modified mica catalyst, J. Mol. Liq. 237 (2017) 38–45.
[59] B.R. Moser, S.F. Vaughn, Evaluation of alkyl esters from Camelina sativa oil as biodiesel and as blend components in ultra-low-sulfur diesel fuel, Bioresour. Technol. Rep. 101 (2010) 646–653.
[60] N.A. Negm, G.H. Sayed, F.Z. Yehia, O.I. Habib, E.A. Mohamed, Biodiesel production from one-step heterogeneous catalyzed process of Castor oil and Jatropha oil using novel sulphonated phenyl silane montmorillonite catalyst, J. Mol. Liq. 234 (2017) 157–163.
[61] M. Lapuerta, O. Armas, R.G. Contreras, Effect of ethanol on blending stability and diesel engine emissions, Energy Fuels 23 (2009) 4343–4354.
[62] J. Lin, T.A. Trabold, M.R. Walluk, D.F. Smith, Bio-fuel reformation for solid oxide fuel cell applications. part 1: fuel vaporization and reactant mixing, Int. J. Hydrog. Energy 38 (2013) 12024–12034.
[63] ASTM D-93-16, Standard Test Methods for Flash Point by Pensky-Martens Closed Cup Tester, (2018).
[64] A. Schuster, W. Friedt, Glucosinolate content and composition as parameters of quality of Camelina seed, Ind. Crops Prod. 7 (1998) 297–302.
[65] G. Knothe, Analyzing biodiesel: standards and other methods, Review. J. Am. Oil Chem. Soc. 83 (2006) 823–833.
[66] N.A. Negm, M.T.H. Abou Kana, M.A. Youssif, M.Y. Mohamed, Biofuels from vegetable oils as alternative fuels advantages and disadvantages, Surfactants Tribol. 5 (2017) 289–367.
[67] P.A.Giuliano S. Albo, H. Lago, P. Wolf, Density, viscosity and specific heat capacity of diesel blends with rapeseed and soybean oil methyl ester, Biomass Bioenergy 96 (2017) 87–95.
[68] M.L. Huber, E.W. Lemmon, A. Kazakov, L.S. Ott, T.J. Bruno, Model for the thermodynamic properties of a biodiesel fuel, Energy Fuels 23 (2009) 3790–3797.